Surface-induced organization of ***n***-alkanes on nanostructured PTFE: I. Brillouin spectroscopic investigations on pentacosane

1996 J. Phys.: Condens. Matter 8 7579

(http://iopscience.iop.org/0953-8984/8/41/007)

J. Phys.: Condens. Matter **8** (1996) 7579–7587. Printed in the UK

Surface-induced organization of n-alkanes on nanostructured PTFE: I. Brillouin spectroscopic investigations on pentacosane

R Jiménez†, J K Krüger, K-P Bohn and C Fischer

Fachrichtung Experimentalphysik 10.2, Universität des Saarlandes, Bau 38, Postfach 151150, D-66041-Saarbrücken, Germany

Received 28 May 1996

Abstract. Taking advantage of the surface-induced orientation of linear molecules on highly oriented nanostructured polytetrafluoroethylene, we were able to grow macroscopic single crystals of $C_{25}H_{52}$ (pentacosane). Using high-performance Brillouin spectroscopy, we determined for the first time the complete elastic tensor of an n-alkane.

1. Introduction

Although the structural properties of $C_{25}H_{52}$ (pentacosane) are well established [1–6], as in the case of other n-alkanes [7], the determination of the elastic properties of the crystalline state was handicapped by the difficulty in obtaining sufficiently defectless single crystals [8]. The typical habit and plasticity of solution- or melt-grown crystals make it difficult to prepare suitable crystal cuts to be used in ultrasonic or Brillouin spectroscopic experiments. The lack of suitable samples did however not hinder the work to obtain preliminary elastic data of these substances although almost only indirect experimental methods were discussed in the literature. Pioneering work was done by Pechhold [9] in polycrystalline paraffins, by Heyer *et al* [10] using the inelastic neutron scattering method developed by Buchenau [11], and by the determination of LAM Raman modes by Strobl and Eckel [12, 13]. Strobl and Eckel were able to calculate from the basic LAM mode and its overtones for $C_{33}H_{68}$ the elastic constant $c_{33} = 41$ GPa, although they found for the crystal lamella a limiting elastic constant, $c_{33}^{\infty} = 289.86$ GPa [12]. This limiting elastic constant, c_{33}^{∞}, was assumed to be the same for all n-paraffins. More recently, Snyder *et al* [14] performed a new analysis of the LAM modes and proposed a chain length dependence of the interlamellar elastic constant c_i.

The first successful application of a direct method to characterize the elastic properties of these materials was performed by Krüger *et al* [15,16] using the Brillouin spectroscopy on a solution growth $C_{36}H_{74}$ single crystal. Unfortunately at that time it was only possible to obtain a reduced set of elastic constants.

Applying the 90A and 90R scattering geometries [17–19] to mesoscopic single-crystalline domains of polycrystalline perfluoroalkanes and semifluorinated alkanes, Marx *et al* [20–22] determined the complete elastic stiffness tensor of the room-temperature phases of these materials.

† Present address: Instituto de Ciencia de Materiales de Madrid (CSIC), Cantoblanco, E-28049-Madrid, Spain.

0953-8984/96/417579+09$19.50

Very recently, we have proposed a preparation method, based on the surface-induced organization of linear molecules on highly oriented nanostructured polytetrafluoroethylene (the polymer-induced alignment (PIA) technique), to obtain oriented crystal plates of *n*-alkanes or perfluoroalkanes. This technique, originally introduced by Wittmann and Smith [23], allows us to obtain oriented crystal mats of very different materials (e.g. polymers [24, 25], liquid crystals [26, 27] and *n*-alkanes and perfluoroalkanes [28, 29]).

The effect of the PTFE (PIA substrate) in *n*-alkanes and perfluoroalkanes is twofold. On the one hand it induces a preferential orientation of the crystallites with the *c*-axis parallel to the preferential orientation of the PIA substrate, and on the other hand this orientation forms a homogeneous crystal mat suitable to be measured by Brillouin spectroscopy. A comparison with other crystal growth techniques has shown that the PIA technique usually provides the same crystal structure. As a matter of fact the PIA technique forces a biaxial orientation of the crystals on the PIA substrate with the crystallographic *c*-axis as well as the *b*-axis within the film plane [28, 29]. The orientation mechanism of linear molecules on this highly oriented substrate is still a matter of intensive investigations [30, 31].

The aim of this work is to present a scenario for how to determine the whole stiffness tensors of *n*-alkanes with help of the PIA technique. As a model system we chose $C_{25}H_{52}$. We will discuss our results in the frame of existing structural data for the room-temperature phase of pentacosane [2, 3, 5, 6].

2. Experimental details

2.1. Sample preparation

The raw material of $C_{25}H_{52}$ was purchased from Applied Science Laboratories Inc. and had commercial purity grade.

The PIA technique to prepare sandwich samples has been described in detail in previous papers [26–29]. Here we want only to stress the most important aspects that are of relevance for the present work. The PTFE (PIA) layer, deposited on a conventional glass slide, is molecularly highly oriented, highly crystalline and has a typical thickness of 10 nm. According to optical and preliminary x-ray investigations [32], the pentacosane–PIA layer composite shows an outstanding biaxial structure with a preferential alignment of the linear alkane molecules along the rubbing direction of the PIA substrate (see e.g. [26–29]). In addition, the crystallographic *b*-axis is preferentially oriented within the film plane. This result is in complete accordance with that previously found for $C_{17}H_{36}$ [28].

In order to overcome the non-wetting effect of PTFE with respect to $C_{25}H_{52}$, and in order to maintain the mono-crystalline structure in 10 μm thick samples, we filled a thin-film glass cuvette with the pentacosane material, having coated the relevant inner faces with PIA (see figure 1). The usual cooling from the melt to room temperature yields cracks, being perpendicular to the preferential direction of the $C_{25}H_{52}$ molecules (the crystallographic *c*-axis). Due to optical and acoustical diffraction, these cracks significantly disturb the Brillouin measurements especially for phonon wave propagation parallel to the *c*-axis. In order to reduce almost all these defects, we applied a modified Bridgman crystal growth technique [33]. This method drastically reduces heteronucleation as well as thermo-mechanical stresses resulting from differences of the thermal expansion coefficients between sample and substrate. In order to obtain free standing samples, we floated the crystalline sample from the glass cuvette. It should be pointed out that the PIA substrates remain on the sample surfaces.

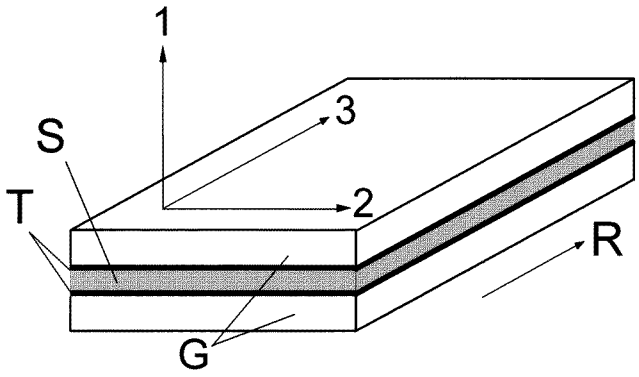

Figure 1. The principle of a PIA sandwich sample: *S*, *n*-alkane sample; T, PTFE layer; G, glass slides; R, rubbing direction of the PTFE layer.

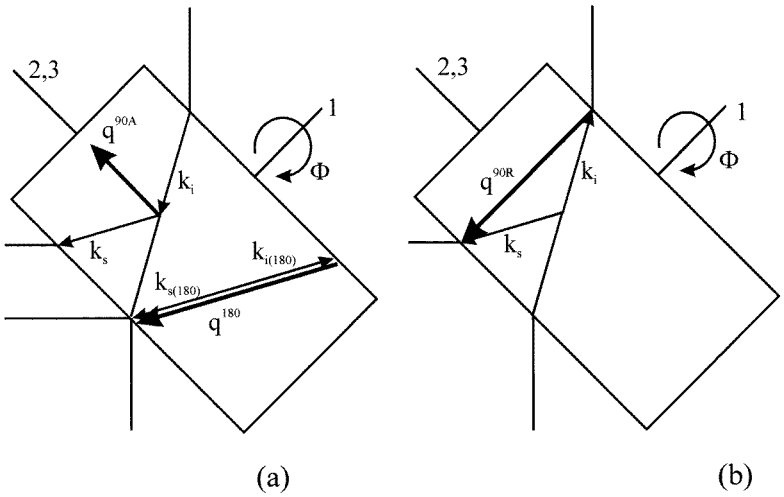

Figure 2. A schematic representation of (a) the 90A and (b) the 90R scattering geometries for a filmlike sample. The sample is rotated around the 1-axis, thus moving $\boldsymbol{q}^{90A}$ within the plane defined by the 2- and 3-axes. $\boldsymbol{q}^{90R}$ is always parallel to the 1-axis. If the sample is very thin, the $\boldsymbol{q}^{180}$ wave vector can also be collected giving the backscattering contribution discussed in the text. $\boldsymbol{k}_i$, incident light wave vector; $\boldsymbol{k}_s$, scattered light wave vector. For further information see the text.

2.2. Brillouin spectroscopy (BS)

The Brillouin spectrometer used is based on a five-pass Fabry–Perot interferometer with an Ar ion laser as light source. The experimental set-up has been described elsewhere (see e.g. [19]). Figure 2 schematically shows the principles of the 90A and 90R scattering geometries [17–19]. Using exclusively filmlike samples angle-resolving BS [34] allows the determination of all or almost all the elastic constants present in the elastic stiffness tensor and of the relevant optical properties of the crystalline state. The relations between sound

velocity, v, and the corresponding phonon frequencies, f^{90A} and f^{90R}, are

$$v^{90A} = f^{90A}\lambda_0/\sqrt{2} \qquad v^{90R} = f_i^{90R}\lambda_0/\sqrt{4n_i^2 - 2} \tag{1}$$

where λ_0 is the laser wavelength in vacuum (514.5 nm in our case) and n_i is the relevant refractive index of the sample. As has been discussed elsewhere, in the case of the 90A scattering geometry, the influence of the birefringence on the acoustic wavelength can be omitted [19]. The stiffness coefficient, c, related to the measured sound velocity obeys the relation $c = \rho v^2$ where ρ is the mass density of the material. Measuring the phonon frequency for different directions of the phonon wave vector $\boldsymbol{q}^{90A}$ within the film plane (see figures 1 and 2), the resulting data can be fitted to the Christoffel equation (see e.g. [35]) yielding the desired stiffness coefficients c_{kl}. The basic relation for the determination of the elastic stiffness tensor $\mathbf{c}$, written in matrix notation, is given by

$$\det(\mathbf{lcl}^T - \mathbf{E}c'(p, \boldsymbol{q})) = 0 \tag{2}$$

with

$$\mathbf{l} = \begin{pmatrix} l_1 & 0 & 0 & 0 & l_3 & l_2 \\ 0 & l_2 & 0 & l_3 & 0 & l_1 \\ 0 & 0 & l_3 & l_2 & l_1 & 0 \end{pmatrix}. \tag{3}$$

$\mathbf{c} = \{c_{kl}\}$ is the fourth-rank elastic tensor in shortened 6×6 Voigt notation; $\mathbf{E}$ is a 6×6 unity matrix; $l_i (i = 1, 2, 3)$ are direction cosines which define the direction of the wave vector $\hat{\boldsymbol{q}} = (l_1, l_2, l_3)$. The right-handed orthogonal co-ordinate system $\{1, 2, 3\}$ is given in figure 1. For the expected orthorhombic symmetry of $C_{25}H_{52}$ at room temperature, the elastic stiffness coefficients are c_{11}, c_{22}, c_{33}, c_{12}, c_{13}, c_{23}, c_{44}, c_{55} and c_{66} (Voigt notation). The indices 1, 2 and 3 refer to the crystallographic axes a, b and c respectively.

The 3-axis points along the $\boldsymbol{c}$-axis of the orthorhombic symmetry of the n-alkane film; the 1-axis is directed orthogonal to the PIA film (crystallographic a-axis, see figure 1). For the (2, 3)-plane (the crystallographic (b, c)-plane) $\hat{\boldsymbol{q}} = (0, \sin\Phi, \cos\Phi)$ holds (see figures 1, 2 and 3).

The relative accuracy of the measured sound frequencies is usually better than 0.5%. The accuracy of the components of the elastic tensor are estimated to be better than 1%.

3. Results and discussion

As usual in the family of odd paraffins, $C_{25}H_{52}$ shows at room temperature orthorhombic symmetry with the space group P_{cam} [1–4]. The lattice parameters are [2]: $\boldsymbol{c} = 67 \pm 0.5$ Å; $\boldsymbol{a} = 7.45 \pm 0.05$ Å and $\boldsymbol{b} = 4.92 \pm 0.05$ Å. The corresponding mass density at room temperature is $\rho = 951.9$ kg m^{-3}.

For the interpretation of the elastic properties of $C_{25}H_{52}$ it is important to know whether our PIA-prepared samples are also representative for melt- or solution-grown crystals. As has been shown in [36], the PIA samples show the same phase transition behaviour as conventional melt- or solution-grown crystals. In addition to this, preliminary x-ray results [31] yield the same lattice constants given above and indicate the same preferential spatial orientation of the crystallographic axes as in the case of $C_{17}H_{36}$ [28].

A first 90A Brillouin measurement was performed on a sample in a glass cuvette internally covered with PIA layers. The corresponding sound velocity data are given in figure 3(a). Unfortunately, for phonon propagation around the c-axis the sound frequency of the longitudinal polarized phonon of $C_{25}H_{52}$ coincides with that of the glass container contributing also to the scattering volume. On the other hand, we obtained a representative

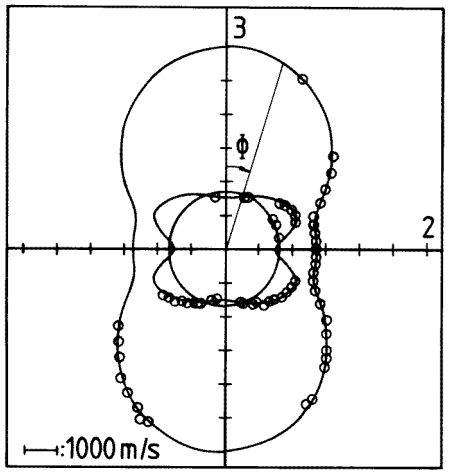

(a)

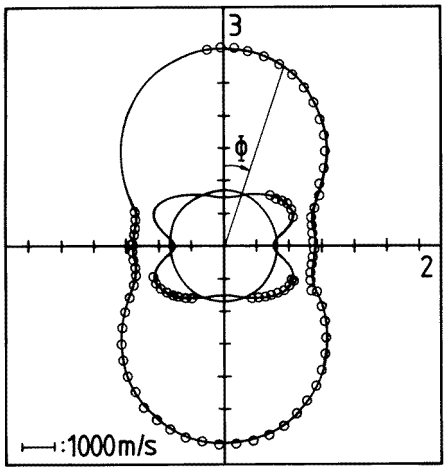

(b)

Figure 3. A polar plot of the three phonon branches within the (2, 3)- plane of the sample (90A scattering). The full lines refer to a least-squares fit of the Christoffel equation (2) assuming orthorhombic symmetry. (a) A PIA film in a glass sandwich; (b) a free-standing PIA film. In both cases the outer curve denotes the quasi-longitudinal branch, the two inner ones the quasi-transverse branch and the transverse branch (circle) respectively.

data set on the quasi-transverse and pure transverse branches which, together with the quasi-longitudinal branch, allowed us to evaluate the stiffness constants c_{22}, c_{33}, c_{23}, c_{44}, c_{55} and c_{66}.

An alternative way to obtain the desired elastic constants is to make the Brillouin measurements on free-standing mono-crystalline films of $C_{25}H_{52}$. The film thickness of the free-standing film was 10 μm, which is small compared to our optical information volume (lateral dimensions of about 50 μm). Then, the scattering volume contains, obviously, only the pentacosane surfaces surrounded by air. Figure 3(b) presents the polar plot of the experimental data on the quasi-longitudinal and quasi-transverse branches. Due to an

increased elastic light scattering because of a slightly reduced surface quality of the free-standing film, we were not able to identify the pure shear phonons.

Comparing the sound frequency data of figure 3(a) and (b) we obtain a very good agreement between the polar diagrams, yielding all the elastic stiffness constants except c_{11}, c_{12} and c_{13}.

The quantitative analysis of the experimental data was performed using the Christoffel's equation (2) in a non-linear least-squares fit assuming orthorhombic symmetry for the $C_{25}H_{52}$ sample. The full lines in figure 3(a) and (b) show the three acoustic branches (transverse, quasi-transverse and quasi-longitudinal) obtained by the non-linear least-squares fit to the data (table 1).

Table 1. Elastic constants and refractive indices of $C_{25}H_{52}$ at room temperature and for comparison those of $C_{33}H_{68}$ found in the literature [13]. Our refractive index values have been measured at a wavelength of 514.5 nm; those of Strobl are n_D values. For further information see text.

	$C_{25}H_{52}$	$C_{33}H_{68}$ [13]
ρ (kg m^{-3})	951.9	952.7
c_{22} (GPa)	7.4	4.415
c_{33} (GPa)	35.0	41.67
c_{23} (GPa)	2.4	—
c_{44} (GPa)	2.1	—
c_{55} (GPa)	2.8	—
c_{66} (GPa)	2.7	—
c_{11} (GPa)	7.2	4.415
c_{13} (GPa)	2.1	—
c_{12} (GPa)	4.1	2.38
c_i (GPa)	3.5	3.1
$n_1^{514.5\ nm}$	1.515	1.523
$n_2^{514.5\ nm}$	1.511	1.519
$n_3^{514.5\ nm}$	1.549	1.588

The determination of the missing elastic constants (c_{11}, c_{12} and c_{13}) needs Brillouin measurements of acoustic modes containing information about the missing tensor components. The stiffness coefficient c_{11} can be determined easily by means of the 90R scattering geometry with the phonon wave vector directed along the crystallographic a-axis, provided that the related refractive index is known. Using an Abbé refractometer we determined $n_1^{514.5\ nm} = 1.515 \pm 0.002$ and $n_2^{514.5\ nm} = 1.511 \pm 0.005$ for the sodium D line at ambient temperature. For immersion we chose a silicone oil ($n_D = 1.578$) which does not chemically attack the $C_{25}H_{52}$ sample. Due to the rather low refractive index of the immersion oil we were not able to measure n_3 (see below). We have measured the f^{90R} frequencies for the electrical field vectors $\boldsymbol{E}$ of the incident and the scattered light either along the b-axis or the c-axis: $f^{90R}(\boldsymbol{E} \parallel 2) = 14.3$ GHz and $f^{90R}(\boldsymbol{E} \parallel 3) = 14.76$ GHz. From $f^{90R}(\boldsymbol{E} \parallel 2)$ together with n_2 we have calculated the sound velocity (1) for phonon propagation along the crystallographic a-axis yielding $v_1 = 2755$ m s^{-1}. Using v_1 and the mass density $\rho = 951.9$ kg m^{-3} we obtained the stiffness value $c_{11} = 7.2$ GPa. In turn, (1) together with $f^{90R}(\boldsymbol{E} \parallel 3) = 14.76$ GHz yields the refractive index $n_3^{514.5\ nm} = 1.549$.

The difference between the refractive index of the sample and that of the surrounding air combined with the small thickness of the PIA film gives rise to strong reflection of the incident laser light as well as of the scattered light on the sample–air interfaces resulting in the well known additional back scattering lines in the recorded spectra [19].

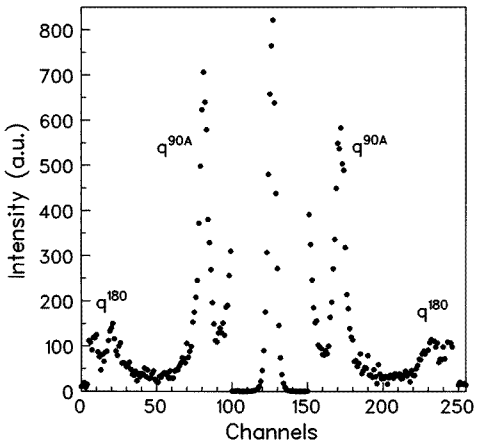

(a)

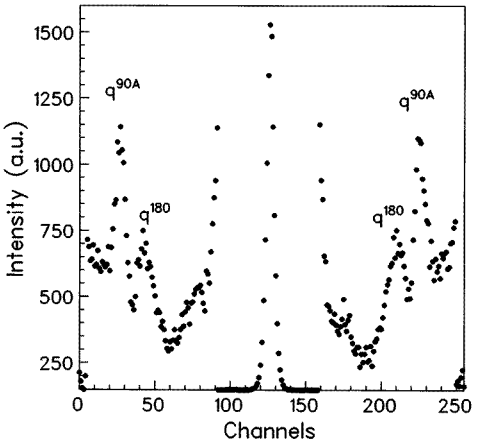

(b)

Figure 4. Typical Brillouin spectra of a $C_{25}H_{52}$ free-standing PIA film sample. (a) $\boldsymbol{q}^{90A}$ parallel to the crystallographic b-axis. (b) $\boldsymbol{q}^{90A}$ parallel to the crystallographic c-axis. The Rayleigh lines (central lines) have been reduced by a factor of 1000 to fit the graphic scales.

Figure 4 shows typical Brillouin spectra in the case of a free-standing film for different orientations of the phonon wave vector, $\hat{\boldsymbol{q}}$, within the PIA sample plane. With help of this additional backscattering process (figure 2) in the free-standing alkane film, it is possible to estimate the remaining elastic constants c_{12} and c_{13}. Using the main refractive indices n_1, n_2 and n_3 together with the outer scattering angle ($\Phi_0 = 45^\circ$) we calculated the inner scattering angles Θ_{i1} and Θ_{i2} and the wave vectors for backscattering within the (a, b)- and (a, c)-planes. Using these scattering vectors together with the measured sound frequencies ($f_{a,b}^{180}(\Theta_{i1}) = 17.5$ GHz and $f_{a,c}^{180}(\Theta_{i2}) = 14.2$ GHz) we calculated the corresponding stiffness moduli $c_{eff}^{a,b}(\Theta_{i1}) = 8.0$ GPa and $c_{eff}^{a,c}(\Theta_{i2}) = 5.2$ GPa respectively. Using these stiffness constants together with those given in table 1, the Christoffel equation (2) yields c_{12} and c_{13} respectively. As has been checked, the complete Voigt matrix $\{c_{ij}\}$ is positive definite.

In order to compare our elastic data with those of $C_{33}H_{68}$ given by Strobl [13] we calculated the compliance matrix for $C_{25}H_{52}$ (see table 2). Taking into account the difference in molecular chain length and some rough assumptions in the calculations of Strobl the agreement between the two data sets seems to be acceptable.

Table 2. The elastic compliance tensor of $C_{25}H_{52}$, and the related values for $C_{33}H_{68}$ [13]. The values in brackets were fixed by Strobl [13].

	$C_{25}H_{52}$	$C_{33}H_{68}$ [13]
ρ (kg m^{-3})	951.9	952.7
S_{22} (Pa^{-1})	2×10^{-10}	3.2×10^{-10}
S_{33} (Pa^{-1})	2.9×10^{-11}	2.4×10^{-11}
S_{23} (Pa^{-1})	-6.6×10^{-12}	(0)
S_{44} (Pa^{-1})	4.7×10^{-10}	—
S_{55} (Pa^{-1})	3.6×10^{-10}	—
S_{66} (Pa^{-1})	3.8×10^{-10}	—
S_{11} (Pa^{-1})	2.0×10^{-10}	3.2×10^{-10}
S_{13} (Pa^{-1})	-4.8×10^{-12}	(0)
S_{12} (Pa^{-1})	-1.1×10^{-10}	-1.7×10^{-10}

As has been discussed earlier [12, 15, 16] the weak interlamellar interactions are responsible for the renormalization of the limiting modulus of the single lamella, c_{33}^{∞}, down to the measured hydrodynamic low value c_{33} (see table 1). Of course, the interlamellar interaction forces are of the van der Waals type. Therefore, it is of interest to compare these interaction forces with those along the crystallographic *a*- and *b*-axes, which are, at least in principle, of the same origin. As a measure for these interactions we take c_{11}, c_{22} and c_i where the latter is an interlayer modulus (see section 1). This interlayer modulus can be estimated roughly using a series connection for the description of the elastic properties for phonon propagation along the *c*-axis (see e.g. [21])

$$c/2c_{33} = L_i/c_i + L_l/c_{33}^{\infty}. \tag{4}$$

$c = 2L_l + 2L_i$ is the crystallographic lattice constant, L_l is the length of the carbon chain (all-*trans* conformation) and L_i is the thickness of the interlamellar region. c is known from x-ray data (see above) and, assuming all-*trans* conformation of the chain, the lamella thickness L_l ($= (n-1) \times 2.545/2$ Å) can be calculated from the related sub-cell parameter. Then L_i can be evaluated from the difference between c and L_l ($2L_i = c - 2L_l$). For c_i we obtain a value of 3.5 GPa (table 1) which is rather close to c_{11} and c_{22}. Indeed, this result reflects the dominant role of the van der Waals forces for the propagation of acoustic waves in *n*-alkanes.

4. Conclusions

Within this work we introduced the PIA technique as a very efficient method of growing macroscopic oriented single crystals of pentacosane, being representative for other *n*-alkanes. The quality of the crystal films allowed us to determine the main refractive indices. Angle-resolving Brillouin spectroscopy permitted, for the first time, the determination of the complete elastic stiffness tensor of an *n*-alkane single crystal of low symmetry. The interlamellar stiffness constant reflects the dominance of the van der Waals forces for the acoustic properties of *n*-alkanes.

Acknowledgments

This work was kindly supported by the Deutsche Forschungsgemeinschaft.

References

[1] Piesczek W, Strobl G R and Malzahn K 1974 *Acta Crystallogr.* B **30** 1278
Strobl G, Ewen B, Fischer E W and Piesczek W 1974 *J. Chem. Phys.* **61** 5257
[2] Denicolò I, Doucet J and Craievich A F 1981 *J. Chem. Phys.* **75** 1523; 1981 *J. Chem. Phys.* **75** 5125; 1983 *J. Chem. Phys.* **78** 1465
[3] Ungar G 1983 *J. Phys. Chem.* **87** 689
[4] Doucet J, Denicolò I, Craievich A F and Germain C 1984 *J. Chem. Phys.* **80** 1647
[5] Sirota E B, King H E, Singer D M and Shao H 1993 *J. Chem. Phys.* **98** 5809
[6] Sirota E B and Singer D M 1994 *J. Chem. Phys.* **101** 10 873
[7] Broadhurst M G 1962 *J. Res. NBS* A **66** 241
[8] Boistelle R 1980 *Current topics in Material Science* vol 4, ed E Kaldis (Amsterdam: North-Holland)
[9] Pechhold W, Dollhopf W and Engel A 1966 *Acoustica* **17** 61
[10] Heyer D, Buchenau U and Stamm M 1984 *J. Pol. Sci.* **22** 1515
[11] Buchenau U 1979 *Solid State Commun.* **32** 1329
[12] Strobl G R and Eckel R 1976 *J. Pol. Sci.* **14** 913
[13] Strobl G R 1976 *Col. Pol. Sci.* **254** 170
[14] Snyder R G, Strauss H L, Alamo R and Mandelkern L 1994 *J. Chem. Phys.* **100** 5422
[15] Krüger J K, Bastian H, Asbach G I and Pietralla M 1980 *Pol. Bull.* **3** 633
[16] Krüger J K, Pietralla M and Unruh H-G 1982 *Phys. Status Solidi* a **71** 493
[17] Krüger J K, Peetz L and Pietralla M 1978 *Polymer* **19** 1397
[18] Krüger J K, Pietralla M and Unruh H-G 1983 *Col. Pol. Sci.* **261** 409; 1982 *Phys. Status Solidi* a **71** 493
[19] Krüger J K, Marx A, Peetz L, Roberts R and Unruh H-G 1986 *Col. Pol. Sci.* **264** 403
[20] Marx A, Krüger J K and Unruh H-G 1988 *Appl. Phys.* A **47** 367
[21] Marx A, Krüger J K and Unruh H-G 1989 *Z. Phys.* B **75** 101
[22] Marx A, Krüger J K, Kirfel A and Unruh H-G 1990 *Phys. Rev.* B **42** 6642
[23] Wittmann J C and Smith P 1991 *Nature* **352** 414
[24] Krüger J K, Prechtl M, Smith P, Meyer S and Wittmann J C 1992 *J. Pol. Sci.* B **30** 1173
[25] Krüger J K, Prechtl M, Wittmann J C, Meyer S, Legrand J F and D'Asseza G 1993 *J. Pol. Sci.* B **31** 505
[26] Grammes C, Krüger J K, Bohn K-P, Baller J, Fischer C, Schorr C, Rogez D and Alnot P 1995 *Phys. Rev.* E **51** 420
[27] Krüger J K, Grammes C, Jiménez R, Schreiber J, Bohn K-P, Baller J, Fischer C, Rogez D, Schorr C and Alnot P 1995 *Phys. Rev.* E **51** 2115
[28] Jiménez R, Krüger J K, Prechtl M, Grammes C and Alnot P 1994 *J. Phys.: Condens. Matter* **6** 10 977
[29] Jiménez R, Krüger J K, Fischer C, Bohn K-P, Dvorák V, Holakovský J and Alnot P 1995 *Phys. Rev.* B **51** 3353
[30] Frey H, Sheiko S, Möller M, Wittmann J C and Lotz B 1993 *Adv. Mater.* **5** 917
[31] Fenwick D, Smith P and Wittmann P C 1996 *J. Mater. Sci.* **31** 128
[32] Servet B 1995 private communication
[33] Krüger J K, Heydt B, Fischer C, Baller J, Jiménez R, Servet B, Galtier P, Pavel M, Ploss B, Bottani C and Beghi M *Phys. Rev.* B submitted
[34] Krüger J K 1989 *Optical Techniques to Characterize Polymer Systems* ed H Bässler (Amsterdam: Elsevier)
[35] Auld B A 1973 *Acoustic Fields and Waves in Solids* (New York: Wiley)
[36] Krüger J K, Jiménez R, Bohn K-P and C Fischer *Phys. Rev.* B submitted